

Neural-network-based modeling and optimization of the electro-discharge machining process

S. Assarzadeh · M. Ghoreishi

Received: 29 November 2006 / Accepted: 10 September 2007 / Published online: 3 November 2007
© Springer-Verlag London Limited 2007

Abstract In this research, a new integrated neural-network-based approach is presented for the prediction and optimal selection of process parameters in die sinking electro-discharge machining (EDM) with a flat electrode (planing mode). A 3–6–4–2-size back-propagation neural network is developed to establish the process model. The current (I), period of pulses (T), and source voltage (V) are selected as network inputs. The material removal rate (MRR) and surface roughness (Ra) are the output parameters of the model. Experimental data were used for training and testing the network. The results indicate that the neural model can predict process performance with reasonable accuracy, under varying machining conditions. The effects of variations of the input machining parameters on process performance are then investigated and analyzed through the network model. Having established the process model, a second network, which parallelizes the augmented Lagrange multiplier (ALM) algorithm, determines the corresponding optimum machining conditions by maximizing the MRR subject to appropriate operating and prescribed Ra constraints. The optimization procedure is carried out in each level of the machining regimes, such as finishing ($Ra \leq 2 \mu\text{m}$), semi-finishing ($Ra \leq 4.5 \mu\text{m}$), and roughing ($Ra \leq 7 \mu\text{m}$), from which, the optimal machining parameter settings are obtained. The optimization results

have also been discussed, verified experimentally, and the amounts of relative errors calculated. The errors are all in acceptable ranges, which, again, confirm the feasibility and effectiveness of the adopted approach.

Keywords Electro-discharge machining (EDM) · Artificial neural network (ANN) · Back-propagation (BP) algorithm · Augmented Lagrange multiplier (ALM) algorithm · Process modeling

1 Introduction

Amongst the nonconventional machining processes, which, nowadays, find a wide range of applications, electro-discharge machining (EDM) is considered to be one of the most important processes for machining intricate and complex shapes in various electrically conductive materials, including high-strength, temperature-resistant (HSTR) alloys, especially in the aeronautical and automotive industries. In EDM, controlled discrete electrical discharges (sparks) provided by a generator, between a tool (electrode) and a work piece submerged in a liquid dielectric medium, are used to remove material by melting and vaporizing the surface layers of the work piece. Since EDM uses high-energy electro-thermal erosion (instead of mechanical cutting forces) and there is no physical contact between the tool and the work piece, the process is not restricted by physical and metallurgical properties of the work material, such as strength, toughness, microstructure, etc. Thus, slender and fragile tasks can also be machined conveniently, making the process more versatile.

Comprehensive qualitative and quantitative analysis of the material removal mechanism and, subsequently, the

S. Assarzadeh
Islamic Azad University of Ghouchan,
P.O. Box 463, Ghouchan, Iran

M. Ghoreishi (✉)
Mechanical Engineering Department,
Khajeh Nasir (K.N.) Toosi University of Technology,
Tehranpars, Vafadar-e-Sharghi St.,
P.O. Box 16765-3381, Tehran, Iran
e-mail: ghoreishi@kntu.ac.ir

development of model(s) of material removal are not only necessary for a better understanding of the process, but are also very useful in parametric optimization, process simulation, operation and process planning, parametric analysis (i.e., understanding the influence of various process parameters on the process performance measures), verification of the experimental results, and improving the process performance by implementing/incorporating some of the theoretical findings [1].

The successful integration of optimization techniques and adaptive control of EDM depends on the development of proper relationships between output parameters and the controllable input variables, but the stochastic and complex nature of the process makes it too difficult to establish such relationships. The erosion by an electric discharge involves phenomena such as heat conduction, melting, evaporation, ionization, formation, and collapse of gas bubbles and energy distribution in the discharge channel. These complicated phenomena, coupled with the surface irregularities of electrodes, interactions between two successive discharges, and the presence of debris particles, make the process too abstruse, so that complete and accurate physical modeling of the process has not been established yet [2, 3].

Most previous theoretical studies have been concerned with microscopic metal removal arising from a single spark, the effects being modeled from heat conduction theory and thermodynamic considerations [4–9]. Although, the models are physically based, due to the random distribution of electrical discharges in the gap space and the overlapping effects of two consecutive sparks on the work piece surface, as well as inevitable assumptions and simplified approaches, which, in turn, push the physical model far away from reality, they can not be generalized to the real multi-spark state of the EDM process [3].

The difficulties of EDM physical modeling have motivated the use of data-driven or empirical methods in which the process is analyzed using statistical techniques. Ghoreishi and Atkinson [10, 11] employed statistical modeling and process optimization for the case of EDM drilling and milling. They compared the results of vibratory EDM, rotary EDM, and a combination of these (vibro-rotary EDM), and concluded that the vibro-rotary electrode compared with the rotary or vibratory cases alone gives satisfactory results when the most usual combination of requirements were considered in an optimization procedure. In another study, Wang and Tsai [12, 13] proposed semi-empirical models for the material removal rate (MRR), surface finish, and tool wear on the work piece and the tool for various materials in EDM, employing dimensional equations based on relevant process parameters for the screening experiments and the dimensional analysis. Although their semi-empirical

models involve thermal, physical, electrical, and material properties of the work piece and the tool in comparison with the other empirical models proposed earlier, the error analysis between predictions and experimental results showed that the models, especially the MRR model, have reasonable accuracy only if the MRR is large, i.e., should the process inputs be in the range of yielding large MRR, the model will be trustable. This reduces the reliability and versatility of their models for use under various machining conditions.

In general, while statistical techniques are useful for identifying general trends in process inputs and outputs, they are subject to a number of disadvantages. Fitting curves to nonlinear data needs the selection of transforms, which, inevitably, is subjective and becomes very difficult when multiple inputs are involved [14]. Also, regression analysis is not well suited to modeling noisy data. These considerations have led to the identification of the neural network approach, which overcomes these difficulties.

Artificial neural networks (ANNs), as one of the most attractive branches in artificial intelligence, has the potential to handle problems such as modeling, estimating, prediction, optimization, diagnosis, and adaptive control in complex nonlinear systems [15]. The capabilities of ANNs in capturing the mathematical mapping between input variables and output features are of primary significance for modeling machining processes. Kao and Tarng [16] and Liu and Tarng [17] have employed feed-forward neural networks with hyperbolic tangent activation functions and abductive networks for the classification and on-line recognition of pulse types. Based on their results, discharge pulses have been identified and then used for controlling the EDM machine. Indurkha and Rajurkar [18] developed a 9–9–2-size back-propagation neural network for orbital EDM modeling. Having compared the results of the neural network model with estimates obtained via multiple regression analysis, they concluded that the neural model is more accurate and also less sensitive to noise included in the experimental data. Although the various effects of changes of input parameters on the process outputs were analyzed and interpreted through the network model, they did not present any way of determining optimal input conditions to optimize the process for an arbitrary desired surface roughness (Ra). Tsai and Wang [19, 20] applied various neural network architectures for the prediction of the MRR and Ra in EDM. Compared with their previous semi-empirical models reported in [12, 13], the selected networks had considerably lower amounts of error, but, nevertheless, the neural models have a lack of generality, since the networks were trained to have just one output of either the MRR or Ra. Therefore, an inadequate model was obtained to estimate both the MRR and Ra simultaneously. Also no discussion was paid to the determination of

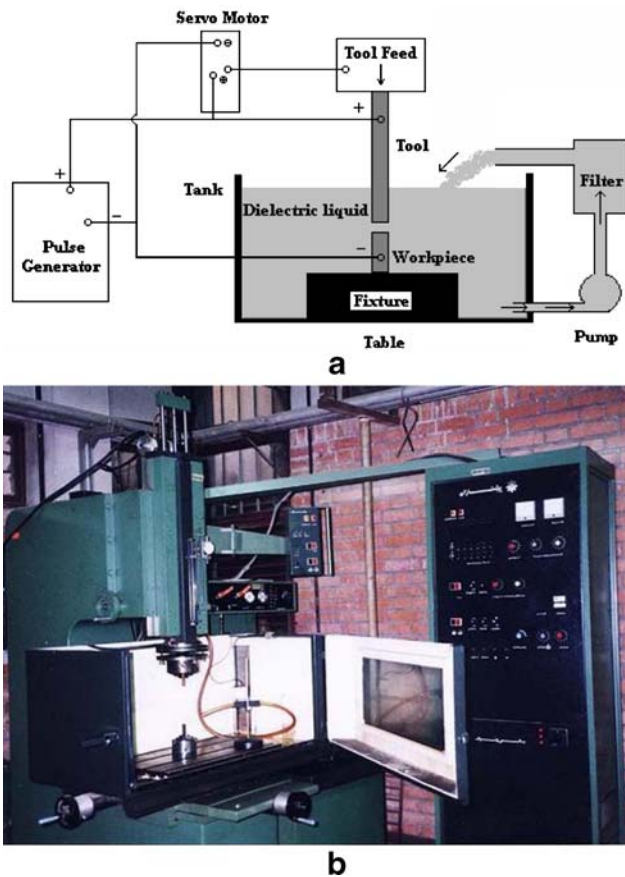


Fig. 1a, b The experimental equipment. **a** Schematic drawing. **b** Photograph of the electro-discharge machining (EDM) machine

operating conditions leading to optimum machining performance.

The purpose of this paper is to present an efficient and integrated approach for the determination of appropriate machining parameters yielding the objective of maximum MRR, and, hence, the shortest machining time, which is very important for the time-consuming EDM process, whilst at the same time, satisfying the requirements of Ra and side constraints on input parameters. First, a back-propagation neural network is developed to establish the process model. Training and testing of the network are performed using experimental data. As a result of modeling, the effects of changes of process input parameters on output features are illustrated and studied. The modeling phase is followed by an optimization procedure, during which, an augmented Lagrange multiplier (ALM) network is used to determine optimal input parameters for the maximum MRR in each machining regime of finishing, semi-finishing, and roughing. The obtained optimal input settings are also interpreted and verified experimentally. Finally, our concluding remarks are outlined.

2 Back-propagation neural network

Since the objective is to evolve a model that relates selected inputs with outputs, so, the back-propagation (BP) neural network constitutes an excellent tool due to its universal approximation capabilities [21]. The BP network is a multiple-layer network with an input layer, output layer, and some hidden layers between the input and output layers.

Before practical application, the network has to be trained so that the free parameters or connection weights are determined, and the mapping between inputs and outputs is accomplished. The training method is called back-propagation [22], a supervised learning technique, which generally involves two phases through different layers of the network; a forward phase and a backward phase. In the forward phase, input vectors are presented and propagated forward to compute the output for each neuron. During this phase, synaptic weights, which are all randomly set to begin with, are fixed and the mean square error (MSE) of all of the patterns in the training set is calculated.

The backward phase is an iterative error reduction performed in the backward direction from the output layer to the input layer. Usually, the gradient descent method, adding a momentum term, is used to minimize the error, MSE, as fast as possible. These two phases are iterated until the weight factors stabilize their values and the mean square error is at a minimum or an acceptably small value.

More details about the mechanism of the training process can be found in [15] and [22].

3 Experimental details

In order to obtain different machining process parameters and output features for the training and testing of the neural network, a series of experiments was performed on a Pishtazan electro-discharge machine (model SP120A) equipped with an iso-frequency pulse generator. A schematic drawing and photograph of the experimental apparatus is shown in Fig. 1.

At first, some preliminary tests were carried out to determine the stable domain of the machine parameters and also the different ranges of process variables. Based on preliminary test results and working characteristics of the

Table 1 Pertinent process parameters and their levels for machining experiments

| Process parameters | Operating conditions |
|----------------------------------|----------------------|
| Discharge current, I (A) | 2, 5, 8, 11, 14, 17 |
| Period of pulses, T (μ s) | 50, 100, 200, 500 |
| Source voltage, V (v) | 35, 50, 60, 70 |

Table 2 The effects of different numbers of hidden neurons on the back-propagation (BP) network performance of a single-hidden-layer network ($\eta_F=0.9$; mean square error (MSE) goal=0.005)

| No. of hidden neurons | Average error in MRR (%) | Average error in Ra (%) | Total average error (%) |
|-----------------------|--------------------------|-------------------------|-------------------------|
| 6 | 11.73 | 4.97 | 8.35 |
| 7 | 11.33 | 7.52 | 9.43 |
| 8 | 9.83 | 7.17 | 8.50 |
| 9 | 16.35 | 5.51 | 10.93 |

EDM machine, the discharge current (I), period of pulses (T), and source voltage (V) were chosen as the independent input parameters. During these experiments, by altering the values of the input parameters to different levels, stable states of the machining conditions have also been specified. Accordingly, the main experiments were conducted with six levels of discharge current, four levels of period of pulses, and four levels of source voltage. Table 1 shows the input process variables and their levels in the experiments.

Throughout the experiments, BD3 steel and commercial copper were used as the work piece and tool electrode materials, respectively. The work pieces were heat-treated up to 58 RC to establish real and practical situations in all tests. Also, the dielectric liquid used was kerosene and the positive terminal of the power supply was linked with the tool electrode (tool: positive polarity, work piece: negative polarity). Particular attention was paid to ensure that the operating conditions permitted the effective flushing of machining debris from the working region. Thus, the experiments were done in the planing process mode, in which the bottom surface of the electrode is flat and parallel to the work piece surface. Also, the diameter of the cylindrical electrode was equal to the diameter of the round bar work piece and was chosen to be 12 mm.

To achieve validity and accuracy, each test was repeated three times. The MRR and Ra were selected as the performance characteristics or process outputs, since the performance of any machining process is evaluated in terms of these two measures. Then, the mean values of the three response measurements (MRR and Ra) were used as the output for each set of parameters. The machining time considered for each test was dependent on the discharge current and much time was allocated to the tests with a lower current.

The MRR was estimated by the weight difference of the work pieces before and after machining using a digital single pan balance (maximum capacity=1,000 g, precision=0.01 g) and are reported in units of g/h. The surface roughness (Ra) was measured by means of a Surtronic 3+, with the Ra value in microns at a cut-off length of 0.8 mm.

The total data obtained from the machining experiments ($6 \times 4 \times 4$) is 96 and these form the neural network's training and

testing sets. The results also show that the training data cover a wide variety of possible ranges, i.e., in our case, the three main groups of finishing ($Ra \leq 2 \mu\text{m}$), semi-finishing ($2 \mu\text{m} < Ra \leq 4.5 \mu\text{m}$), and roughing ($Ra > 4.5 \mu\text{m}$) are involved.

Finally, it should be mentioned that the adopted planing mode of machining did help reduce the tool wear rate (TWR) greatly, so that its amount was less than 0.001 g accuracy of weight. If another mode, e.g., drilling, was selected for the experiments, the TWR could manifest itself noticeably [23].

4 BP neural network modeling of the EDM process

Modeling of the EDM process with a BP neural network is composed of two stages: training and testing of the network with experimental machining data. The training data consist of values for current (I), period of pulses (T), and source voltage (V), and the corresponding MRR and Ra. In all, 96 such data sets were used, of which, 82 data sets were selected randomly and used for training purposes, while the remaining 14 data sets were presented to the trained network as new application data for verifying or testing the predictive accuracy of the network model. Thus, the network was evaluated using data that had not been used for training.

4.1 Data preprocessing

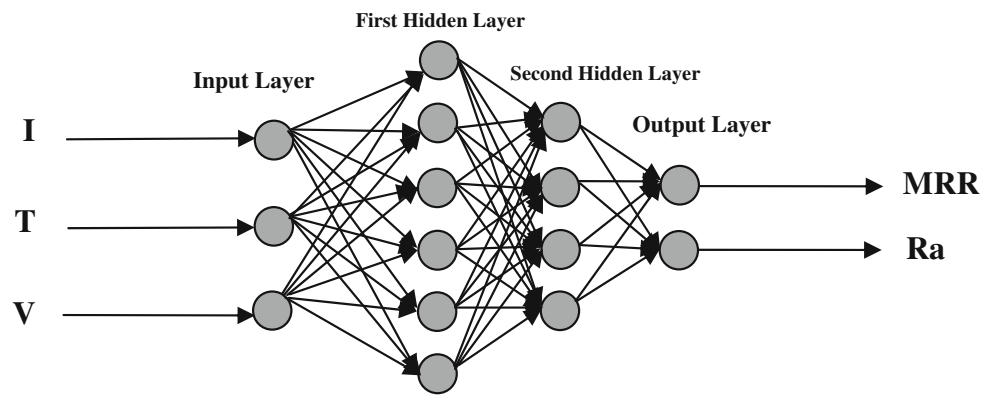
Before the ANN can be trained and the mapping learnt, it is important to process the experimental data into patterns. Training/testing pattern vectors are formed. Each pattern is formed with an input condition vector, \mathbf{P}_i :

$$\mathbf{P}_i = \begin{bmatrix} \text{Current (I)} \\ \text{Period of pulses (T)} \\ \text{Voltage (V)} \end{bmatrix}$$

Table 3 The effects of different numbers of hidden neurons on the BP network performance of a double-hidden-layer network ($\eta_F=0.9$; MSE goal=0.005)

| No. of neurons in the first hidden layer | No. of neurons in the second hidden layer | Average error in MRR (%) | Average error in Ra (%) | Total average error (%) |
|--|---|--------------------------|-------------------------|-------------------------|
| 5 | 3 | 9.38 | 7.18 | 8.28 |
| | 4 | 12.29 | 6.14 | 9.22 |
| | 5 | 11.67 | 6.10 | 8.89 |
| 6 | 4 | 5.31 | 4.89 | 5.10 |
| | 5 | 8.06 | 6.42 | 7.24 |
| | 6 | 16.20 | 7.58 | 11.89 |

Fig. 2 Configuration of the back-propagation (BP) neural network model for the EDM process



and the corresponding target vector, \mathbf{T}_i :

$$\mathbf{T}_i = \begin{bmatrix} \text{Material removal rate (MRR)} \\ \text{Surface roughness (Ra)} \end{bmatrix}$$

The scale of the input and output data is an important matter to consider, especially when the operating ranges of process parameters are different. The scaling or normalizing ensures that the ANN will be trained effectively, without any particular variable skewing the results significantly. As a result, all of the input parameters are equally important in the training of the neural network. The scaling is performed by mapping each term to a value between -1 and 1 using the following equation:

$$N = \frac{(R - R_{\min}) \times (N_{\max} - N_{\min})}{(R_{\max} - R_{\min})} + N_{\min} \quad (1)$$

where N is the normalized value of the real variable, $N_{\min} = -1$ and $N_{\max} = 1$ are the minimum and maximum values of the normalization, respectively, R is the real value of the

variable, and R_{\min} and R_{\max} are the minimum and maximum values of the real variable, respectively.

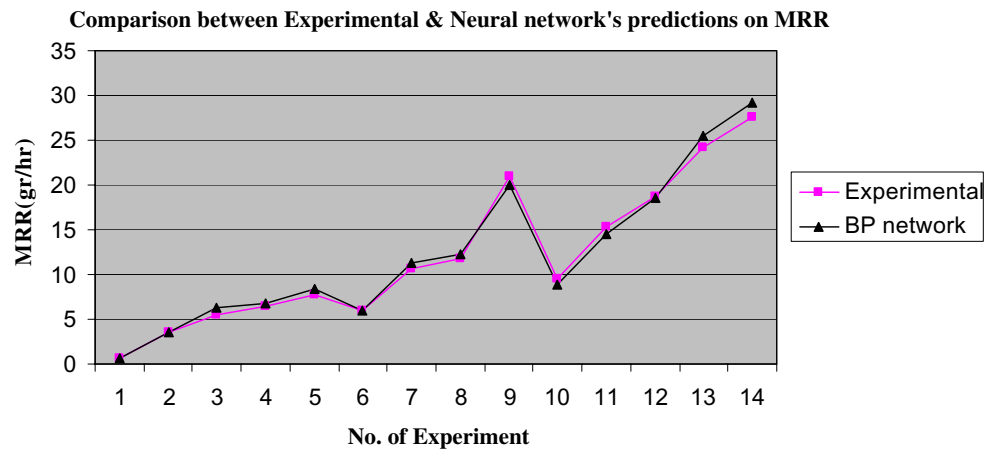
4.2 Network topology, training, and testing

The network has three inputs of current (I), period of pulses (T), and source voltage (V), and two outputs of MRR and Ra. The size of the hidden layer(s) is one of the most important considerations when solving actual problems using multi-layer feed-forward network. To find the best network model that gives superior results in comparison with other networks topologies, a number of candidate networks with different hidden layers and neurons were developed using the Neural Network Toolbox (NNET) of the MATLAB software package. Single- and double-hidden-layer networks with various hidden nodes were trained separately and their performances checked. In other words, the best model, is selected based on its predictive accuracy in response to new input data in the testing phase when compared with experimental values. The results for one- and two-hidden-layer networks having different

Table 4 Comparison of the MRR and Ra measured and predicted by the BP neural network model

| Test no. | Machining conditions | | | MRR (gr/hr) | | Ra (μm) | | Relative error (%) | |
|----------|----------------------|---------------------|-------|--------------|----------|----------------------|----------|--------------------|-------------|
| | I (A) | T (μs) | V (v) | Experimental | BP model | Experimental | BP model | Error in MRR | Error in Ra |
| 1 | 5 | 500 | 35 | 0.70 | 0.71 | 3.05 | 2.68 | 1.43 | 12.13 |
| 2 | 5 | 100 | 50 | 3.54 | 3.61 | 3.28 | 3.35 | 1.98 | 2.13 |
| 3 | 8 | 50 | 70 | 5.45 | 6.26 | 4.27 | 4.32 | 14.86 | 1.17 |
| 4 | 8 | 200 | 50 | 6.39 | 6.83 | 4.52 | 4.48 | 6.89 | 0.88 |
| 5 | 8 | 50 | 60 | 7.72 | 8.41 | 4.85 | 4.90 | 8.94 | 1.03 |
| 6 | 11 | 500 | 70 | 5.97 | 6.03 | 4.92 | 5.23 | 1.01 | 6.30 |
| 7 | 11 | 100 | 70 | 10.64 | 11.34 | 5.25 | 5.74 | 6.58 | 9.33 |
| 8 | 11 | 200 | 60 | 11.83 | 12.30 | 5.45 | 6.08 | 3.97 | 11.56 |
| 9 | 11 | 200 | 35 | 21.01 | 19.92 | 6.9 | 6.60 | 5.19 | 4.35 |
| 10 | 14 | 500 | 50 | 9.52 | 8.85 | 5.12 | 5.29 | 7.04 | 3.32 |
| 11 | 14 | 50 | 50 | 15.3 | 14.57 | 6.1 | 6.13 | 4.77 | 0.49 |
| 12 | 14 | 100 | 60 | 18.64 | 18.57 | 7.3 | 6.95 | 0.38 | 4.79 |
| 13 | 17 | 50 | 35 | 24.27 | 25.51 | 7.2 | 6.47 | 5.11 | 10.14 |
| 14 | 17 | 100 | 35 | 27.51 | 29.22 | 7.32 | 7.26 | 6.22 | 0.82 |

Fig. 3 Comparison of the MRR between the verification and experimental results

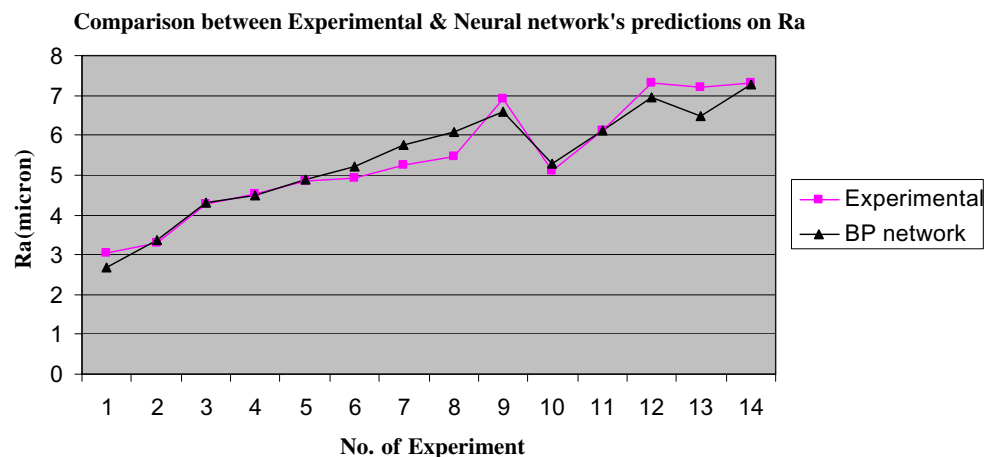


combinations of hidden nodes are shown in Tables 2 and 3, respectively. To train each network, an equal learning rate and momentum constant of $\eta=\alpha=0.9$ was used, the activation function of hidden and output neurons was selected as a hyperbolic tangent, and the error goal (mean square error, MSE) value was set at 0.005, which means that training epochs are continued until the MSE fell below this value. As the error criterion for all networks is the same, their actions are comparable. From Table 2, it is concluded that a total average error of 8.35% is achievable in the best case of a single hidden layer with six neurons, which is generally less than that of the errors belonging to other networks in its group. However, when two hidden layers were tested, a 3–6–4–2-size network gave the best results, reducing average errors the most, compared to other trials. The selected network has mean errors of 5.31% and 4.89% in predicting the MRR and Ra, respectively, over the 14 experimental test data sets. Thus, it has a total average error of 5.10%. This neural model is the best amongst the other competitors of different networks architectures, possessing the least amount of verification errors. The configuration of the neural network model developed is illustrated in Fig. 2. Table 4 shows the experimental and

predicted values for the MRR and Ra, as well as the percentage relative errors in the verification cases. Good agreement between the neural predictions and experimental verifications has been demonstrated in those machining conditions. Figures 3 and 4 also show the comparison of experimental results and modeling in verifying the network generalization capabilities. Figure 5 illustrates the convergence of the output error (MSE) with the number of iterations (epochs) during the training of the best chosen BP network. After 25,908 epochs, the MSE requirement is met, training is stopped, and the weight values of the network are stored. At the beginning of the training, the output from the network is far from the target value. However, the output slowly and smoothly converges to the target value with more epochs, and the network learns the input/output relation of the training samples.

As a further step for studying the capabilities of the model in fitting all points in the input space, a linear regression between the network responses and the corresponding target (experimental) values was performed. In this case, the entire data sets (training+testing) were put through the trained network model, and regression analysis was done. The results are presented separately for the two

Fig. 4 Comparison of the Ra between the verification and experimental results



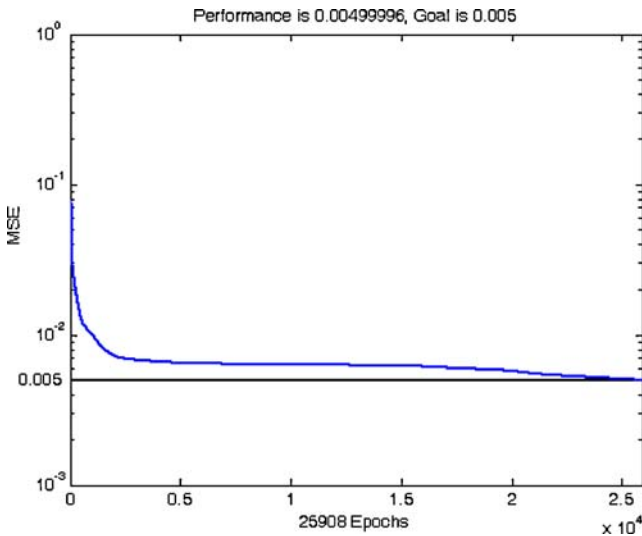


Fig. 5 Learning behavior of the BP neural network model

output parameters in Fig. 6. The correlation coefficients (R) are 0.994 and 0.989 in simulating the MRR and Ra, respectively. From a statistical point of view, the closer this number is to 1, the more powerful the network in correlating the input space to the output space. Therefore, the adopted BP neural network can be used to acquire a function that maps input parameters to the desired process outputs in a wide range of machining conditions.

4.3 Influences of machining parameters on machining performance

In general, both the MRR and Ra depend on the spark energy crossing the discharge gap, and is expressed as $E = \int_{t_p} V_{dis} I dt$. Thus, the process outputs are functions of the discharge voltage, current, and pulse-on time parameters. To separate the effect caused by each machining parameter, the other input variables are set to a constant value in the allowable working spaces when one of the machining parameters is varied and analyzed. In the following, the effects of the machining parameters on the process outputs will be discussed one by one using the developed BP neural network model. Then, by considering the actual circumstances occurring in practice, overall interpretations are drawn. It should also be noted that, in this section, the input values to the neural network are different from those in the experimental data set, so as to fully exploit the generalization capabilities of the model in predicting process behavior under various machining conditions.

4.3.1 Effect of discharge current

The effect of current on EDM characteristics (MRR and Ra) is shown in Figs. 7 and 8, respectively, under the

condition of different pulse periods and a constant 55-v source voltage.

At all values of pulse period, both the MRR and Ra increase steadily with the increase of the current. This was expected, because the MRR and Ra depend on the spark energy, which is directly proportional to the intensity of the

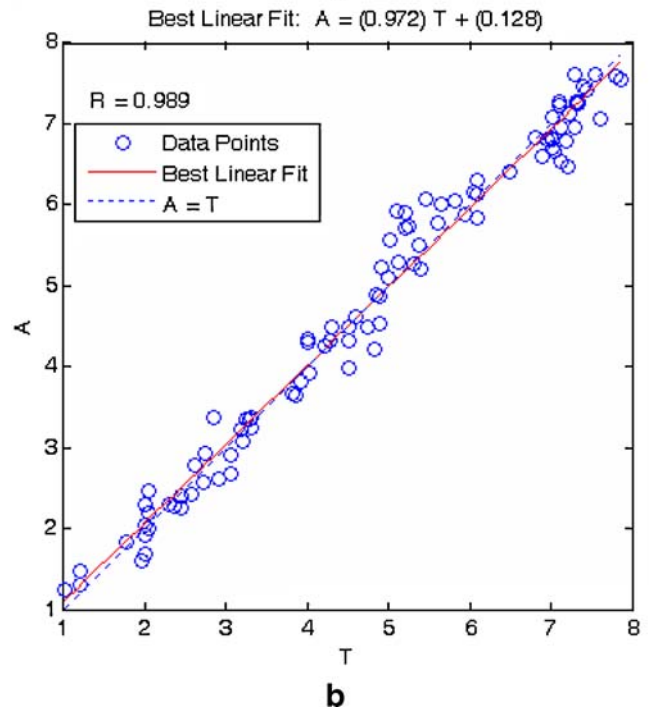
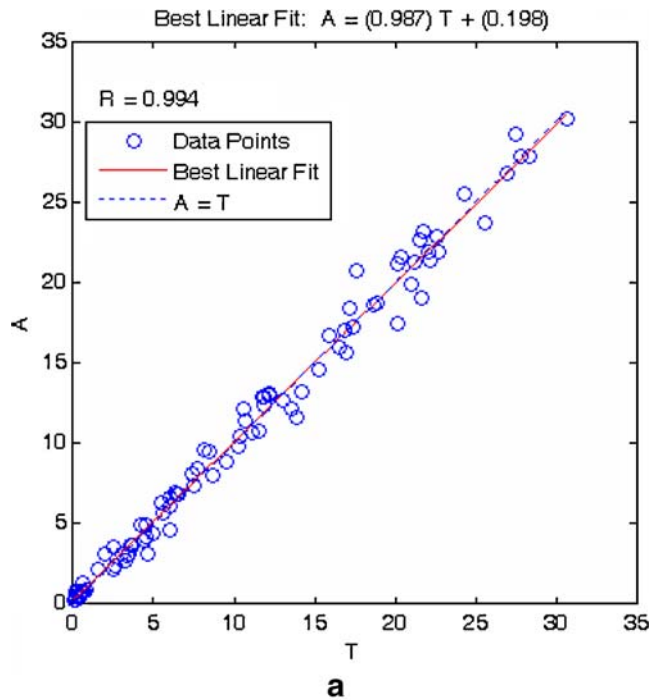
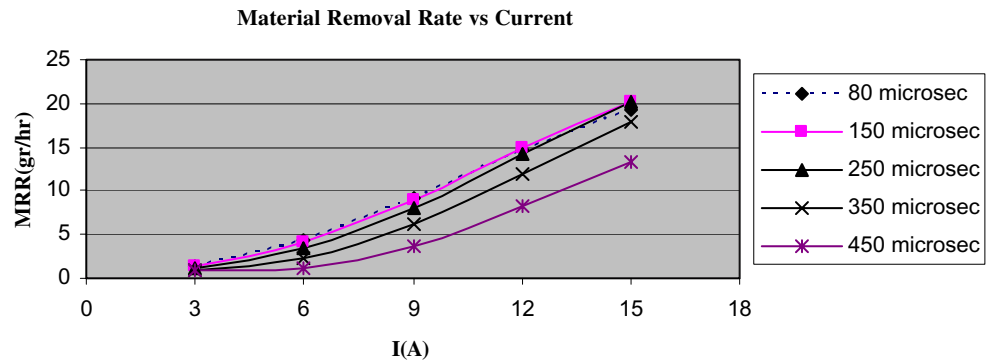


Fig. 6a, b Linear regression analysis between BP network outputs and experimental values. a MRR. b Ra

Fig. 7 Effect of current on the MRR ($V=55\text{ v}$)



current. Therefore, increasing the current results in a greater discharge energy, rising MRR, and leading to poor surface quality.

4.3.2 Effect of pulse period

The effect of the pulse period (pulse-on time+pulse-off time) on the MRR and Ra is depicted in Figs. 9 and 10, respectively, for various source voltage settings at a constant current of 9 A. It is shown that the values of MRR and Ra are highest with a pulse period of about 150 μs . However, with longer pulse periods, the MRR and Ra decrease. This can be explained from the fact that, although spark energy increases with increasing pulse-on time, too long a pulse period causes unfavorable heat losses in the gap space, which does not contribute to the material removal. Therefore, keeping other factors constant, there is an optimum value of pulse period in which the highest MRR occurs.

4.3.3 Effect of source voltage

The effect of source voltage on the MRR and Ra is illustrated in Figs. 11 and 12, respectively, for different current values at a constant pulse period of 250 μs . There are slight changes in the MRR and Ra with respect to source voltage variations. In other words, the source voltage in the

working domain considered in the experiments has not influenced the MRR and Ra considerably.

In brief, the following points can be mentioned as the main findings of a modeling attempt resulting from studying the input parameter variations on the output features considered in the EDM process:

- The discharge current is the most influential or dominant variable among the other input parameters, so that increasing the current with a constant level of pulse period and source voltage increases the MRR and Ra steadily. A high discharge energy associated with high current is capable of removing a chunk of material, leading to the formation of a deep and wide crater, and, hence, worsening the machined surface quality.
- For the effect of pulse period, initially, it is observed that, for all values of source voltage and a constant current, the MRR and Ra increase with increasing pulse period, but these trends continue until about 150- μs pulse period, in which, the MRR gains its maximum value. Although increasing pulse period and, hence, pulse-on time, results in a greater discharge energy, with too long pulse durations, the results become reverse. This is mainly due to the undesirable heat dissipation phenomena of thermal energy liberated during discharge, which, in turn, lessens the erosive effects of sparks.

Fig. 8 Effect of current on the Ra ($V=55\text{ v}$)

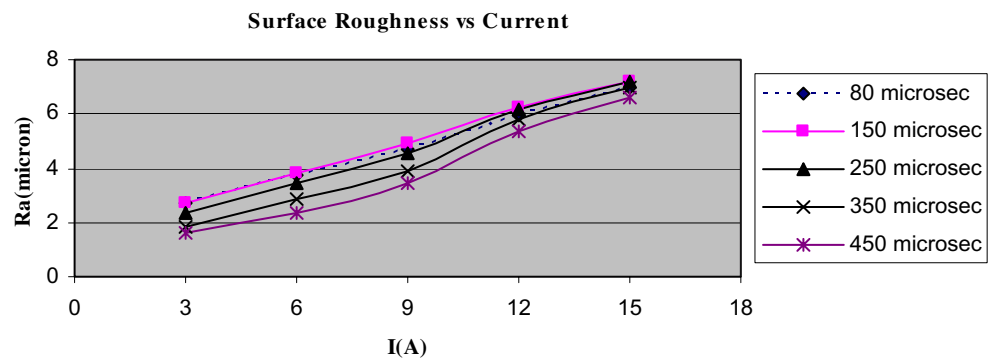
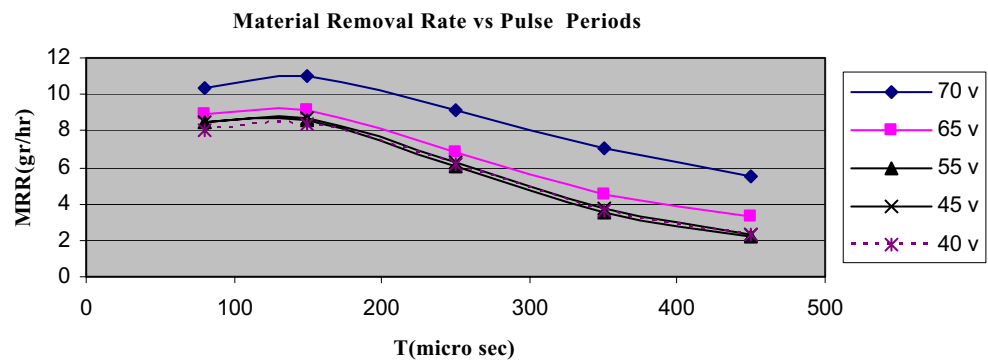


Fig. 9 Effect of pulse period on the MRR ($I=9$ A)



- In normal EDM, the discharge voltage (V_{dis}), influenced primarily by the electrode and work piece materials, is somehow constant, so that an increase in source voltage will have little effect on the discharge energy for a given pair of electrode–work-piece materials. Therefore, increasing the source voltage alone does not necessarily confirm the availability of high discharge voltage, which directly affects the MRR and Ra.

5 Optimization using a neural network

Nonlinear constrained programming is a basic tool in systems where a set of design parameters are optimized subject to inequality constraints. In this section, it is discussed how a trained multi-layered neural network (process model) can be used to optimize a performance index. In the optimization phase, the parameters of the network which have been known as a result of training are kept fixed and the inputs should be adjusted so that the objective function, designated as F , is minimized (or maximized) subject to certain constraints. The key point is to find the partial derivatives of the objective function F with respect to the input data, not the partial derivatives of the error E with respect to the parameters of the network as in the modeling phase.

The ALM neural network [24] is, essentially, a method attached to a punishing function, utilizing an iterative process to find the optimal input parameters in accordance with the prescribed constraints. In the EDM process, the

objective function $F(X)$, which is to be minimized, is the negative of the MRR and the constraint $G(X)$ is on the Ra, which should be less than or equal to the maximum allowable Ra, corresponding to each machining regime. The solution to the above problem is a locally optimal set of process input variables.

The optimization by neural network is simply an optimization procedure with two important differences: no assumption of the input–output model is made and the computations required for the optimization procedure are made in parallel.

Figure 13 shows the general procedure for the modeling and optimization of the EDM process using the two aforementioned neural networks. The partial derivatives of F and G with respect to the input variables x_i can be calculated by using the back-propagation pass performed on the trained network (neural model of the process). This assistance can considerably reduce the computing time in solving the optimization problem. Detailed mathematical explanations of this technique have been given in [25].

6 Determination of optimum machining parameters

What EDM machine manufacturers and users want is to achieve higher machining productivity with a desired accuracy and surface finish. In other words, the higher the MRR and the smoother the surface, the better. But, unfortunately, the goals of high metal removal rate and

Fig. 10 Effect of pulse period on the Ra ($I=9$ A)

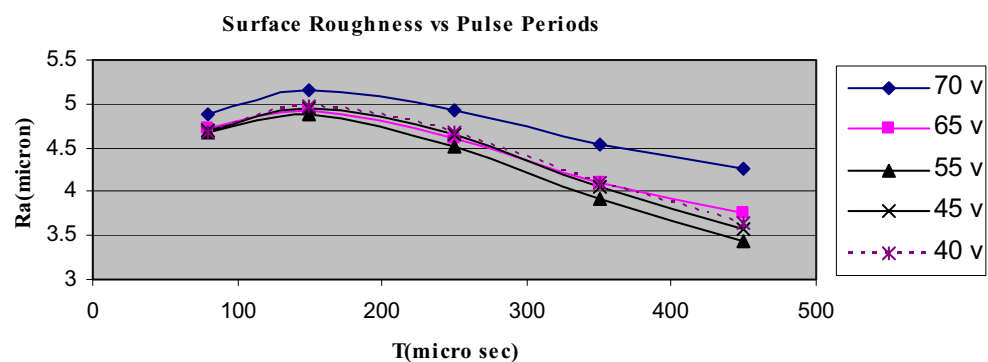
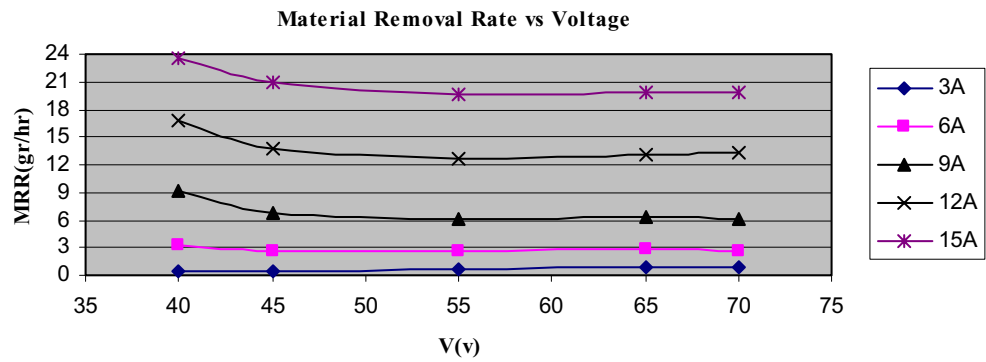


Fig. 11 Effect of source voltage on the MRR ($T=250 \mu s$)



high surface finish quality are, to some extent, conflicting. Consequently, no particular combination of machining parameters can be expected to result simultaneously in the best MRR as well as the best Ra under all circumstances. Therefore, the present problem must be considered to be a multi-objective optimization problem.

To determine the optimum machining conditions, the goals have to be taken separately in different phases of work with different emphasis, i.e., three machining regimes of finishing, semi-finishing, and roughing with relevant prescribed constraints on the Ra need to be considered, and then the optimization procedure (maximizing MRR) is performed in each working domain. Here, the objective function $F(X)$, which should be minimized, is the negative of the MRR (hence, the MRR is maximized) and the constraint $G(X)$ is on the Ra. Assuming that $X=[x_1, x_2, x_3]=[I, T, V]$, then, mathematically, the problem is expressed as:

$$\begin{aligned} \min : F(X) &= -MRR \\ \text{subject to : } G(X) &= Ra \leq Ra_{max} \\ 2 \leq x_1 &\leq 17 \\ 50 \leq x_2 &\leq 500 \\ 35 \leq x_3 &\leq 70 \end{aligned}$$

The Ra_{max} values are $2 \mu m$, $4.5 \mu m$, and $7 \mu m$ for the finishing, semi-finishing and roughing regimes, respectively.

Also, the limitations on the input parameters were assigned according to the experimental setup and electrical capacity of the EDM machine generator described in Sect. 3. Before performing the optimization procedure, it should be noted that the $Ra \leq Ra_{max}$ constraint is always active, since, based on the physics of the process, high MRR results in coarser surface quality. This fact is shown in Fig. 14. Also, from this figure, it is concluded that the optimization problem can yield several locally optimal solutions for some Ra_{max} values. The ALM network starts with an initial point in the input space and converges to a local optimum solution. Furthermore, the graphs of the objective and constraint functions, which are shown in Fig. 15, at a constant current (9 A), indicate that the variation trends of the two functions with respect to the other parameters (T and V) are smooth. Therefore, to find global optimum solutions in each machining case, the optimization process should be repeated several times with different starting points, so as to fully assure that the obtained point is globally optimal. Among all of the possibly obtained candidates of optimal input parameters, the setting which gives the highest MRR and meets the constraint requirements is selected as the global optimum point in each machining regime.

Using the MATLAB software package, an optimization program based on the algorithm described in Sect. 5 was developed, and, in conjunction with the neural network

Fig. 12 Effect of source voltage on the Ra ($T=250 \mu s$)

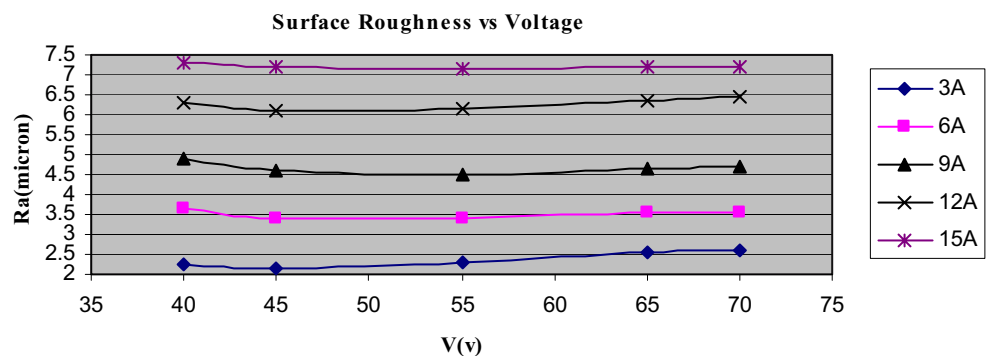
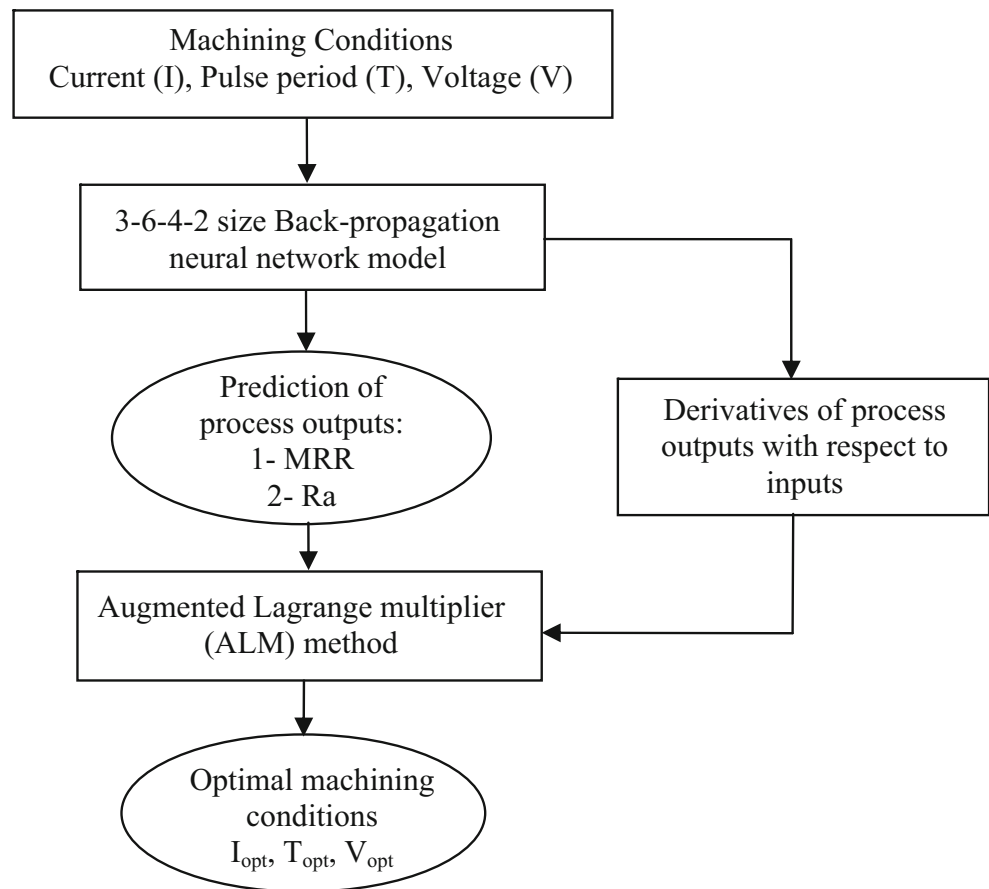


Fig. 13 General procedure adopted for the modeling and optimization of the EDM process



model program, all of the optimum points were found. Table 5 shows the final optimization results. As expected, current intensity increases steadily from the finishing regime to roughing, so that more discharge energy is

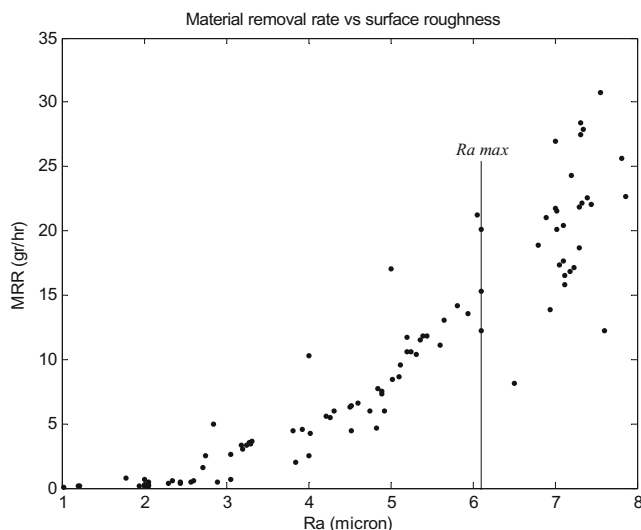


Fig. 14 The Ra constraint is always active and there can exist a locally optimum set of input parameters for some Ra_{max} values

provided, and, therefore, the MRR is enhanced. Especially in the roughing regime, when the surface finish quality is not so important, a maximum MRR has been obtained with almost the highest current (16.96 A). As was explained in Sect. 4.3, it is once more revealed that the discharge current is the dominant factor among the other two input parameters, since the optimum voltages and pulse periods of the semi-finishing and roughing regimes are almost the same, and here, the current is the only variable that has increased to yield maximum MRR, subject to the corresponding constrained Ra. Again, in the finishing regime, as the current is low, the optimal pulse period and voltage have changed in such a way that the maximum MRR of 0.84 g/h is obtained. In this case, the voltage has increased to 59 v, which is higher than the other two optimum voltages in semi-finishing and roughing, to compensate for attaining the maximum MRR. This also leads to a wider gap distance, which facilitates a flushing action, and prevents process instability. For the effect of pulse period, it was shown in Fig. 7 that, at a constant level of source voltage, lower pulse durations, along with higher discharge currents, result in a higher MRR. Therefore, the optimum values of pulse period in the semi-finishing and

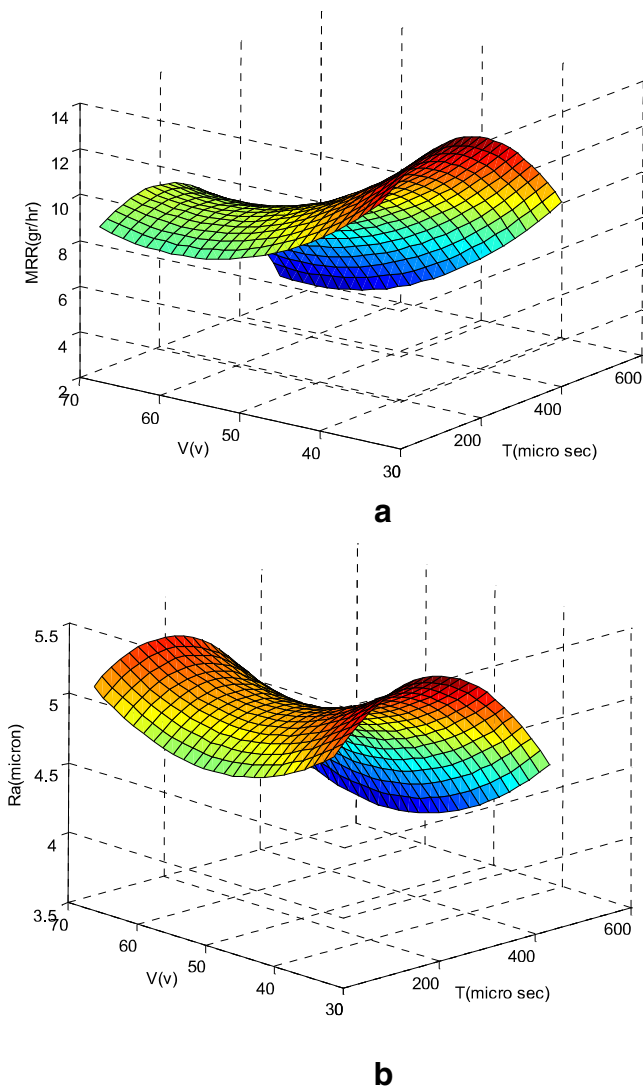


Fig. 15 Three-dimensional surface plots of the objective (a) and constraint (b) functions at a current of 9 A

roughing regimes were found to be the least allowable amount in the machining conditions (50 μs).

Finally, confirmation experiments were conducted to verify the optimization results. The error values, which are

all less than 8%, are also given in Table 5. This proves that the ALM neural network possesses sufficient knowledge in order to perform optimization.

7 Conclusions

In this study, a new approach to optimizing the machining conditions in electro-discharge machining (EDM) for achieving maximum metal removal subject to appropriate operating constraints on the surface roughness (Ra) and machining variables has been presented. As no single combination of input parameters can be optimal for both the material removal rate (MRR) and surface finish (Ra), this led to the notion of separating each level of machining regime based on surface quality emphasis. First, a 3–6–4–2-size back-propagation (BP) neural network model was developed to enable the measures of performance (MRR and Ra) to be predicted in terms of three different control parameters of current (I), pulse period (T), and source voltage (V). Then, an augmented Lagrange multiplier (ALM) neural network is used for determining the optimum parameter settings in each machining regime. The integrated BP-ALM neural network system is fairly general and can be used as a powerful paradigm for the modeling and optimization of any kind of machining process, e.g., electro-chemical machining. The superiority of this approach is highly noticeable when there is only experimental data which demonstrate the process behavior, and little or no explicit mathematical relationships based on the physics of the process are available to correlate the input and output parameters.

Based on the simulation and verification results, the following conclusions can be drawn:

1. The effectiveness of using the BP neural network model for the prediction of the MRR and Ra in the EDM process has been proved.
2. An appropriately trained neural network model along with the ALM neural network can successfully synthe-

Table 5 Final optimization results of the EDM process in different machining regimes

| Machining regime | Optimum setting | | | Responses in optimum conditions | | | | Relative error | |
|--------------------------------|-----------------------|-------------------------|------------------------|---------------------------------|------------|--------------|------------|---------------------|--------------------|
| | | | | ALM network | | Experimental | | | |
| | Current I (2–17) A | Period T (50–500) μs | Voltage V (35–70) v | MRR (g/h) | Ra (μm) | MRR (g/h) | Ra (μm) | Error in MRR (%) | Error in Ra (%) |
| Finishing: Ra ≤ 2 μm | 5.67 | 500 | 59.72 | 0.84 | 2 | 0.87 | 2.14 | 3.45 | 6.54 |
| Semi-finishing: Ra ≤ 4.5 μm | 9.55 | 50 | 35.83 | 13.02 | 4.5 | 13.31 | 4.69 | 2.18 | 4.05 |
| Roughing: Ra ≤ 7 μm | 16.96 | 50 | 35 | 24.89 | 7 | 24.17 | 7.55 | 2.98 | 7.28 |

size optimal input conditions for the EDM process. The optimal input settings maximize the MRR, subject to necessary process constraints.

3. An important aspect is that process optimization can be implemented in the absence of an analytical process model and purely by observations of experimental information.

Following this research, regarding the capability of this method in solving multi-objective optimization problems, the EDM drilling case will be studied by taking the tool wear rate (TWR) and electrodes' corner wear, as well as the corner radius at the bottom surface of the hole as additional constraints, into consideration.

References

1. Jain NK, Jain VK (2001) Modeling of material removal in mechanical type advanced machining processes: a state-of-art review. *Int J Mach Tools Manufact* 41(11):1573–1635
2. Schumacher BM (2004) After 60 years of EDM the discharge process remains still disputed. *J Mater Process Technol* 149:376–381
3. McGeough JA (1988) *Advanced methods of machining*. Chapman and Hall, London, New York
4. Van Djick F (1973) *Physico-mathematical analysis of the electro-discharge machining process*. PhD thesis, Catholic University of Leuven, Belgium
5. Erden A, Kaftanoglu B (1980) Heat transfer modeling of electric discharge machining. In: *Proceedings of the 21st International Machine Tool Design and Research (MTDR) Conference*, Swansea, UK, September 1980, pp 351–358
6. Jilani ST, Pandey PC (1982) Analysis and modeling of EDM parameters. *Precis Eng* 4(4):215–221
7. Erden A, Arinç F, Kögmen M (1995) Comparison of mathematical models for electric discharge machining. *J Mater Process Manuf Sci* 4:163–176
8. Singh A, Ghosh A (1999) A thermo-electric model of material removal during electric discharge machining. *Int J Mach Tools Manufact* 39(4):669–682
9. Katz Z, Tibbles CJ (2005) Analysis of micro-scale EDM process. *Int J Adv Manuf Technol* 25:923–928
10. Ghoreishi M, Atkinson J (2001) Vibro-rotary electrode: a new technique in EDM drilling—performance evaluation by statistical modeling and optimisation. In: *Proceedings of the 13th International Symposium for Electromachining (ISEM XIII)*, Bilbao, Spain, May 2001, pp 633–648
11. Ghoreishi M, Atkinson J (2002) A comparative experimental study of machining characteristics in vibratory, rotary and vibro-rotary electro-discharge machining. *J Mater Process Technol* 120:374–384
12. Wang P-J, Tsai K-M (2001) Semi-empirical model on work removal and tool wear in electrical discharge machining. *J Mater Process Technol* 114:1–17
13. Tsai K-M, Wang P-J (2001) Semi-empirical model of surface finish on electrical discharge machining. *Int J Mach Tools Manufact* 41(10):1455–1477
14. Smith LN, German RM, Smith ML (2002) A neural network approach for solution of the inverse problem for selection of powder metallurgy materials. *J Mater Process Technol* 120:419–425
15. Freeman JA, Skapura DM (1992) *Neural networks: algorithms, applications, and programming techniques*. Addison Wesley, Reading, Massachusetts
16. Kao JY, Tarn YS (1997) A neural-network approach for the on-line monitoring of the electrical discharge machining process. *J Mater Process Technol* 69:112–119
17. Liu HS, Tarn YS (1997) Monitoring of the electrical discharge machining process by abductive networks. *Int J Adv Manuf Technol* 13:264–270
18. Indurkha G, Rajurkar KP (1992) Artificial neural network approach in modeling of EDM process. In: *Proceedings of the Artificial Neural Networks in Engineering (ANNIE'92) Conference*, St. Louis, Missouri, November 1992, pp 845–850
19. Tsai K-M, Wang P-J (2001) Comparisons of neural network models on material removal rate in electrical discharge machining. *J Mater Process Technol* 117:111–124
20. Tsai K-M, Wang P-J (2001) Predictions on surface finish in electrical discharge machining based upon neural network models. *Int J Mach Tools Manufact* 41(10):1385–1403
21. Hornik K, Stinchcombe M, White H (1989) Multilayer feed-forward networks are universal approximators. *Neural Netw* 2(5): 359–366
22. Fausett LV (1994) *Fundamentals of neural networks: architectures, algorithms, and applications*. Prentice-Hall, Englewood Cliffs, New Jersey
23. Assarzadeh S (2003) Modeling of material removal rate and surface roughness in electro-discharge machining (EDM) process using artificial neural networks (ANNs). MS thesis, Department of Mechanical Engineering, Khajeh Nasir (K.N.) Toosi University of Technology, Tehran, Iran
24. Vanderplaats GN (1984) *Numerical optimization techniques for engineering design: with applications*. McGraw-Hill, New York
25. Assarzadeh S, Ghoreishi M (2005) Electro-discharge machining (EDM) process optimization using neural networks. In: *Proceedings of the Tehran International Congress on Manufacturing Engineering (TICME 2005)*, Tehran, Iran, December 2005, pp 12–15